Giant phonon softening in the pseudogap phase of the quantum spin system TiOCl

P. Lemmens,[1,2] K. Y. Choi,[3] G. Caimi,[4] L. Degiorgi,[4,5] N. N. Kovaleva,[1] A. Seidel,[6] and F. C. Chou[6]
[1]*Max Planck Institute for Solid State Research, D-70569 Stuttgart, Germany*
[2]*Institute for Semiconductor Physics and Optics, TU Braunschweig, D-38106 Braunschweig, Germany*
[3]*Institute for Materials Research, Tohoku University, Katahira 2–1–1, Sendai 980–8577, Japan*
[4]*Laboratorium für Festkörperphysik, ETH Zürich, CH-8093 Zürich, Switzerland*
[5]*Paul Scherrer Institute, Ch-5232 Villigen, Switzerland*
[6]*Center for Materials Science and Engineering, MIT, Cambridge, Massachusetts 02139, USA*
(Received 7 July 2003; published 29 October 2004)

Giant anomalies are found in the temperature dependence of Raman-active phonons in the quantum magnet TiOCl, suggesting the presence of an extended fluctuation regime. This regime coincides with a pseudogap phase identified in earlier NMR experiments. The observed large, local spin-gap is proposed to origin from coupled spin/lattice fluctuations. Below 100 K, in the long-range crystallographically distorted phase, a dimerized ground state with a smaller, global spin-gap of about $2\Delta_{spin} \approx 430$ K exists. This transition also marks a dimensionality cross-over of the system.

DOI: 10.1103/PhysRevB.70.134429 PACS number(s): 78.30.−j, 75.10.Jm, 75.30.Et

I. INTRODUCTION

Recently a new class of spin-1/2 transition metal oxides has been identified based on Ti^{3+} ion in a distorted octahedral coordination of oxygen and/or chlorine.[1–4] Such compounds especially in two dimensions (2D) are candidates for exotic electronic configurations[5] and for superconductivity based on dimer fluctuations.[4,6] Their low-energy degrees of freedom are characterized by spin-1/2 quantum magnetism with a singlet ground state as a result of a phase transition. Some of these aspects are reminiscent of a spin-Peierls instability.[7] However, significant differences from such a scenario show up as an extended fluctuation regime above the transition temperature and an extremely large magnitude of the singlet-triplet excitation spin-gap. Therefore, it is tempting to assign part of the dynamics of these phenomena to large electronic energy scales, associated with orbital degrees of freedom. This idea stems from the orbital degeneracy of t_{2g} states of the Ti^{3+} ions ($3d^1, s=1/2$) in octahedral surrounding and from the fact that their orbital ordering can be destabilized by quantum fluctuations.[8,9] Furthermore, novel mechanisms, based on the creation of a coherent spin-orbital structure,[10–12] have been predicted in order to obtain a spin-gap state and coupled spin-orbital modes. Since the lattice is strongly coupled to the orbital state, pronounced phonon anomalies are also expected. Up to now for none of the discussed titanates[1–4] a combined study of the spin and phonon excitation spectrum is available. This is related to the problem of growing sufficiently large single crystals for spectroscopic studies.

In this article we present a Raman scattering and infrared (IR) absorption study on high quality single crystals of insulating TiOCl. We demonstrate an unusual coupling of the electronic degrees of freedom to the lattice which is manifested by giant anomalies in the phonon spectrum, developing over a broad temperature interval known as the pseudogap phase of the compound.[13]

II. STRUCTURAL ASPECTS AND INSTABILITIES OF TiOCl

TiOCl is a 2D oxyhalogenide formed of $Ti^{3+}O^{2-}$ bilayers, separated by Cl^- bilayers. The basic $TiCl_2O_4$ octahedra build an edge-shared network in the *ab*-plane of the orthorhombic unit cell of the FeOCl-type structure.[4,14] Above 100 K the magnetic susceptibility $\chi(T)$ of TiOCl is only weakly temperature dependent.[5] For $T > 200$ K $\chi(T)$ can be fitted using an $s=1/2$ Heisenberg spin chain model with an AF exchange coupling constant $J=660$ K (Ref. 4). Furthermore, $\chi(T)$ displays a sharp drop and a kink at $T_{c1}=66$ K and $T_{c2}=94$ K (Refs. 4, 13, and 15), respectively. The first order phase transition at T_{c1} involves a static structural component with a doubling of the unit cell along the *b*-axis.[15] The sudden loss of susceptibility is connected to the opening of a spin-gap. In band structure calculations a 1D exchange path has been identified along the *b*-axis given by direct exchange of Ti d_{xy} states and superexchange via oxygen and chlorine that hybridize considerably with Ti. The other two d_{xz} and d_{yz} Ti orbitals are degenerate and shifted to higher energies.[4,14] The dominant antiferromagnetic exchange is partially based on these additional superexchange paths. As these paths also connect Ti-sites of chains on the upper and lower bilayer they contribute to a 2D character of the spin system. This scenario makes TiOCl an unique system to study the effect of coupled spin/lattice fluctuations on a topology with competing exchange paths.

The first microscopic information about these fluctuations came from NMR/NQR experiments[13] on ^{35}Cl and $^{47,49}Ti$. The relaxation rate of ^{35}Cl sites indicates dynamic lattice distortions for temperatures below ≈ 200 K. For the $^{47,49}Ti$ sites, $(TT_1)^{-1}$, which probes the spin degrees of freedom, reaches a maximum at $T^*=135$ K. This temperature dependence implies a pseudogap phase in the homogeneous state of the spin system with an estimated pseudogap $\Delta_{fluct} \approx 430$ K (Ref. 13). This gap is extraordinarily large when compared to the transition temperatures, leading to

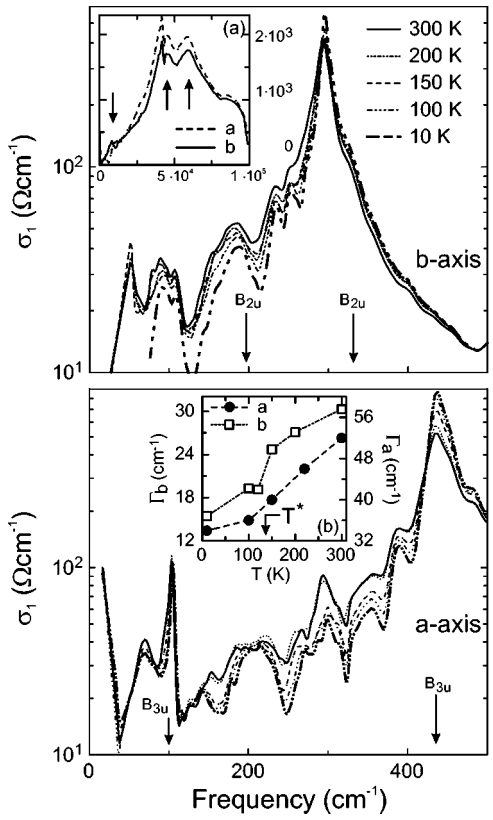

FIG. 1. Real part $\sigma_1(\omega)$ of the optical conductivity (absorption spectrum) of TiOCl as a function of temperature along the *b*-axis and the *a*-axis. The inset (a) shows $\sigma_1(\omega)$ up to the ultraviolet at 300 K. The inset (b) displays the temperature dependence of the width (Γ) of the phonon modes at 294 and 438 cm^{-1}, respectively.

$2\Delta_{\mathrm{fluct}}/k_BT_c=9.1$ and 13, for T_{c2} and T_{c1}, respectively. These ratios are not consistent with a spin-Peierls mechanism.[7]

III. EXPERIMENT

Raman scattering with 514.5 nm excitation wavelength and optical reflectivity $R(\omega)$ experiments have been performed with light polarization within the *ab*-plane of the plateletlike single crystals of TiOCl (Ref. 4). No resonance effects have been detected comparing 514.5 and 488 nm excitation wavelength. The Kramers-Kronig transformation of $R(\omega)$ allows us to evaluate the real part $\sigma_1(\omega)$ of the optical conductivity. Details pertaining to the optical experiments can be found elsewhere.[16,17] Due to the D_{2h} point group symmetry and an inversion center in TiOCl, Raman spectroscopy and optical reflectivity complement each other. In the present scattering geometry they exclusively probe in-plane and out-of-plane (*c*-axis) displacements, respectively.

IV. RESULTS AND DISCUSSION

The real part $\sigma_1(\omega)$ of the optical conductivity (Fig. 1) in the far infrared spectral range shows a strong anisotropy within the *ab*-plane, indicative of the low dimensionality of TiOCl. The inset (a) displays the absorption spectrum up to the ultraviolet spectral range at 300 K, and emphasizes the energy interval dominated by the electronic interband transitions. The observed peak at $\sim$8100 cm^{-1} (1 eV) as well as maxima between 3.2×10^4 and 5.6×10^4 cm^{-1} (4 and 7 eV) (down-arrow and up-arrows in inset (a) of Fig. 1) are interpreted as the charge gap due to the predicted splitting of the t_{2g} orbitals, and the interband transitions between the O and Cl *p*-levels and the Ti *d*-levels, respectively.[4] The $\sigma_1(\omega)$ spectra above 2×10^4 cm^{-1} are polarization independent.

In the far-infrared (main panels of Fig. 1) $\sigma_1(\omega)$ is dominated by strong peaks at 294 cm^{-1} and at 438 cm^{-1} along the *b*-axis and the *a*-axis, respectively. Considering the space group *Pmmn*(59) of TiOCl at room temperature and light polarization in the *ab*-plane, two B_{3u} modes polarized along the *a*-axis and two B_{2u} modes along the *b*-axis are expected as infrared active phonons. Our shell model calculations predict the B_{3u} phonons at 100 and 431 cm^{-1} and the B_{2u} ones at 198 and 333 cm^{-1} (see down-arrows in Fig. 1), which roughly agree with features in our spectra.[16] The larger number of broad and less intense modes are attributed to a lower symmetry than assumed so far as the anisotropy of the optical spectra allows us to exclude twinning or leakage effects of the polarizer. The two strongest modes at 294 cm^{-1} and at 438 cm^{-1} display a narrowing of their linewidth Γ with decreasing temperature (inset (b) of Fig. 1). There is a 49% and 35% decrease[16] of Γ between 300 and 10 K along the *b*- and *a*-axis, respectively. This line narrowing is rather similar to the findings in α'-NaV_2O_5 (Ref. 18) and suggests an extended fluctuation regime.[13,19] The spectral changes occur in the temperature interval of the pseudo spin-gap phase identified in the NMR spectra.[13] There is a depletion of $\sigma_1(\omega)$ over a spectral range of roughly 300–400 cm^{-1} with decreasing temperatures (Fig. 1). Sum rule analysis (Ref. 16 for details) suggests a redistribution of spectral weight from the frequency range below about 400 cm^{-1} up to 1000 cm^{-1}.

For Raman scattering with the light polarized within the ab-plane three phonon modes are expected for the *Pmmn*(59) space group. These A_g modes have only displacements along the *c*-axis of the unit cell and are predicted at 247, 333, and 431 cm^{-1} within the shell model calculation. The Raman spectra with (*aa*) and (*bb*) polarization, shown in the lower inset of Fig. 2, indeed display three modes at 203, 365, and 430 cm^{-1}, denoted by β, γ, and δ, respectively.The response in (*bb*) polarization, parallel to the chain direction of the t_{2g} orbitals, is dominated by quasielastic ($E\approx0$)scattering and a very broad scattering continuum with a maximum at about 160 cm^{-1}, denoted by α. As the temperature dependence of the Raman scattering intensity in the other polarizations is not so pronounced in the following we will concentrate on the (*bb*) polarization.

Quasielastic scattering with Lorentzian line shape observed in (*bb*) polarization is proposed to be due to low-dimensional energy fluctuations of the spin systems.[17] This scattering intensity scales with T^2 multiplied by the specific heat of the spin system. Therefore, it is rapidly suppressed below 300 K, as seen in Fig. 2. Also the linewidth of the α mode strongly decreases. In addition, the maximum of the α mode softens down to 130 cm^{-1}, i.e., by $\approx$20%. In the inset

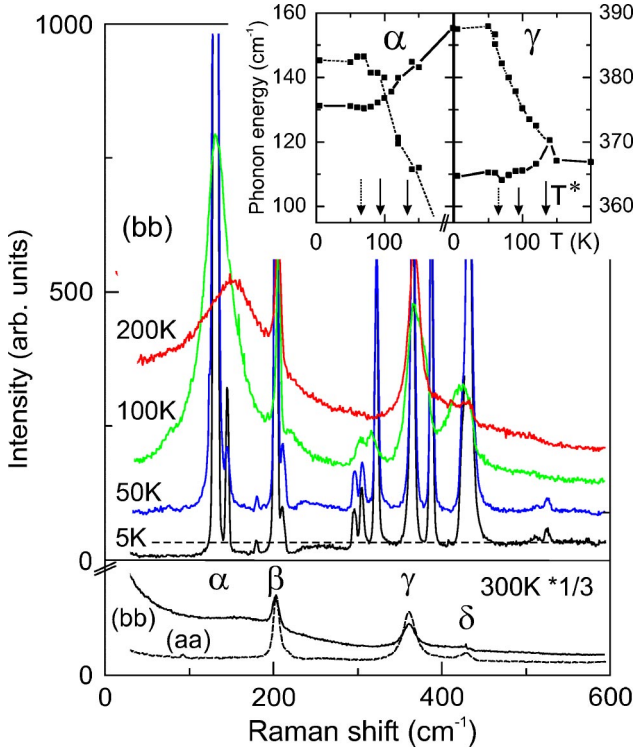

FIG. 2. (Color online) Raman scattering intensity as a function of temperature in (*bb*) polarization and with an offset for clarity. A dashed line extrapolates the scattering at high energies to lower energies ($T=5$ K) to emphasize a spectral depletion for energies below ≈ 300 cm^{-1}. The lower inset compares (*bb*) and (*aa*) polarization at $T=300$ K with the intensity reduced by a factor 1/3. Four important modes are denoted by α to δ. The upper inset shows mode energies on heating the sample. The arrows mark T_{c1}, T_{c2}, and T^*. Modes connected by dashed lines have a smaller intensity.

of Fig. 2 the frequency dependence of the α and γ mode is shown as a function of temperatures together with arrows that denote the characteristic temperatures. The remarkably large softening of the α mode occurs in the fluctuation regime identified by NMR between 200 K and T_{c1}. The energy of this mode is moreover comparable to the spin fluctuation temperature T^*. Also the other modes change appreciably by splitting into several sharp components as shown in the inset. The splitting of the γ mode is definitely observed for temperatures $T>T_{c2}$. For $T<T_{c1}$, however, all transition-induced modes have a sharp and comparable linewidth and no more anomalies are observed. This is especially true for the α mode which cannot be distinguished from the Raman-allowed phonon modes.

In the low-energy range and for $T<T_{c1}$, a depletion of a weak continuum of scattering is visible. This effect is better noticeable when extrapolating the scattering intensity from higher energies, as shown by the dashed line for the $T=5$ K data. It has an approximate onset at 300 cm^{-1} ≈ 430 K, in rough agreement with a similar energy scale obtained from spectral changes[16] in the IR absorption spectra (Fig. 1). Since similar effects have been observed in NaV_2O_5 and $Sr_{14}Cu_{24}O_{41}$ at the double spin-gap of the systems, see, e.g., Ref. 17, we also attribute this onset in TiOCl to $2\Delta_{\text{spin}}=300$ cm^{-1}. The spin-gap $2\Delta_{\text{spin}}$ is about a factor of 2 smaller

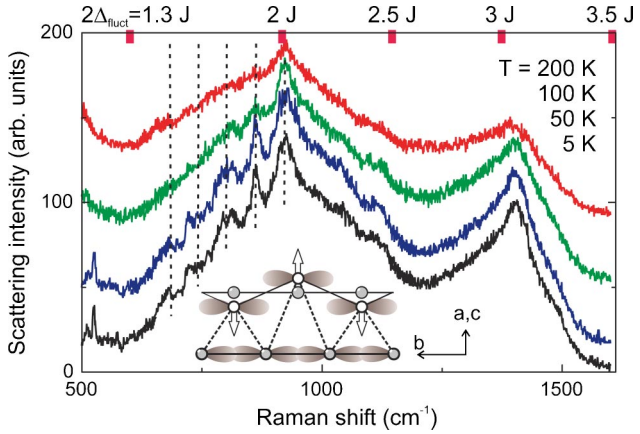

FIG. 3. (Color online) High energy Raman scattering intensity in (*bb*) polarization and an offset for clarity. The inset shows a Ti^{3+}-displacement corresponding to the α-phonon mode. The d_{xy} orbitals with direct overlap form a chain, while dashed lines represent d_{xz} and d_{yz} orbitals.

than the pseudogap $2\Delta_{\text{fluct}}$ determined by NMR[13] and would lead to more reasonable gap ratios of $2\Delta_{\text{spin}}/k_BT_c=4.6$ and 6.7, for T_{c2} and T_{c1}, respectively.

Figure 3 shows the Raman scattering intensity in the high energy range comparable to the exchange coupling constant J. Two maxima are observed, a symmetric one at $2J$ and an asymmetric one at frequencies corresponding to $3J$, respectively, with $J=660$ K determined from magnetic susceptibility.[4] This scattering has also a quite remarkable low-energy onset at ≈ 1.3 J and a cut-off at ≈ 3.4 J. The first maximum ($2J$) resembles the two-magnon continuum of the spin tetrahedra system $Cu_2Te_2O_5Br_2$, which is in the proximity to a quantum critical point.[20,21] As a result strong magnon-magnon interactions lead to a renormalization of the spectral weight and a line shape not compatible with classical long-range ordered magnets. The second maximum ($3J$) is not expected within a simple spin Hamiltonian[17] and might be related to the competition of direct Ti-Ti and more 2D superexchange paths via oxygen and chlorine.[14] Its higher energy ($3J$) would be consistent with a larger coordination number of the involved magnetic sites expected in 2D. In the stripe ordered phase of $(La,Sr)_2NiO_4$ a similar two-peak structure has been observed and attributed to exchange processes along and across stripe domains.[22] There is no pronounced temperature dependence of the two-magnon scattering with the exception of a moderate reduction in intensity. This is related to the comparably large exchange coupling and that no changes of the involved orbital states are present in this temperature range. The onset of magnetic Raman scattering at 600 cm^{-1} ≈ 860 K ≈ 1.3 J is identified as the lowest energy of local spin-pair excitations, similar to observations in other quantum magnets (Refs. 20 and 21). This excitation gap is identical in energy and in its weak temperature dependence to the pseudogap $2\Delta_{\text{fluct}}$ observed in NMR.[13] For Raman shifts $\Delta\omega \lesssim 2J$ a modulation with a characteristic energy of 60–70 cm^{-1} is observed and marked by dotted vertical lines in Fig. 3. This frequency corresponds quite well to the energy separation between the β mode and the α mode at lowest temperatures. Such an effect implies an effective

modulation of the exchange coupling by the two modes. A somewhat comparable signature has been observed in $Sr_{14}Cu_{24}O_{41}$ due to a charge ordering-induced modulation of the exchange coupling in the spin ladders.[23]

The fluctuation or pseudogap regime is characterized by the large nonlinear softening of the α mode and the strong coupling of this mode to the spin excitation spectrum. All observations point to a phonon as the origin of the α mode. As the symmetry-allowed modes (β, γ, δ) have all been observed and the large intensity of the α mode is not consistent with a smaller, local symmetry breaking, we attribute the α mode to the Brillouin zone boundary. The β mode is its related zone center Raman-allowed phonon due to its close proximity in energy. Lattice shell model calculations show that the respective displacement is a pure *c*-axis in-phase Ti-Cl mode. A projection of the corresponding zone-boundary displacements onto two adjacent Ti chains leads to an alternating deflection of the Ti sites out of the *b*-axis chain (see inset of Fig. 3). A band structure calculation using frozen phonons has shown that exactly these displacements strongly couple to the Ti and hybridized oxygen and chlorine states and locally reverse the scheme of the Ti states. The higher lying t_{2g}, d_{xz}, and d_{yz} states, that mediate the exchange perpendicular to the chains, are admixed to the ground state and the respective hopping matrix elements are enhanced.[14] Such a coupling of low and high energy scales via the quasi-degenerate orbitals is a general property of the discussed t_{2g} systems.[1–4]

Finally, we discuss the sequence of characteristic temperatures, T_{c1}, T_{c2}, and the spin fluctuation temperature T^*. While with decreasing temperatures ($T \leqslant T^*$) the coherence length of the structural distortion slowly increases, the magnetic correlations crossover from 2D to 1D due to a change of the t_{2g} orbital admixture. This is the reason for the essentially temperature independent susceptibility, meaning that an increase of magnetic correlations is compensated by a depopulation of the α-β phonon branch. The energy gain for $T \leqslant T_{c2}$ is mainly related to the spin system. Therefore anomalies in the specific heat are small[15] and in conventional x-ray scattering no sign of a coherent structural distortion can be found.[19] The structural distortions become long range only for $T \leqslant T_{c1}$ as a consequence of an order-disorder transition based on spin-lattice coupling.[14] Below this temperature the system can be regarded as a dimerized spin chain system with a global spin-gap $2\Delta_{spin}$. In the short-range-ordered, pseudogap phase there exist a larger spin-gap $2\Delta_{fluct}$ as a smallest energy for a local double-spin-flip. Therefore, it is not related to the transitions at T_{c1} and T_{c2}.

V. CONCLUSION

The extended spin fluctuation regime of the Ti^{3+} bilayer system TiOCl is proposed to origin from the population/depopulation of a Raman-active phonon that strongly couples to competing direct exchange and superexchange paths. This mode with an energy comparable to the spin fluctuation temperature T^* leads to a dimensionality crossover of the spin subsystem. TiOCl realizes an exceptional example of coupled spin/lattice fluctuations and the observed phenomena might have implications for other correlated systems with spin and orbital fluctuations. Such systems also recently gained importance with respect to the investigation of orbital liquids[8,10,11] and the reconsideration of electron-phonon coupling in high temperature superconductors.[24]

ACKNOWLEDGMENTS

The authors acknowledge fruitful discussions with C. Gros, R. Valenti, T. Saha-Dasgupta, H. Rosner, R. Kremer, A. Perucchi, V. Gnezdilov, B. Batlogg, H. Thomas, P.A. Lee, and B. Keimer. This work was supported by the MRSEC Program of the National Science Foundation under Award No. DMR 02-13282, DFG SPP1073, NATO PST.CLG.9777766, INTAS 01-278, and the Swiss National Foundation for Scientific Research.

[1] E. A. Axtell, T. Ozawa, S. M. Kauzlarich, and R. R. P. Singh, J. Solid State Chem. **134**, 423 (1997).
[2] M. Isobe, E. Ninomiya, A. V. Vasil'ev, and Yu. Ueda, J. Phys. Soc. Jpn. **71**, 1423 (2002).
[3] M. Isobe and Y. Ueda, J. Phys. Soc. Jpn. **71**, 1848 (2002).
[4] A. Seidel, C. A. Marianetti, F. C. Chou, G. Ceder, and P. A. Lee, Phys. Rev. B **67**, 020405 (2003).
[5] R. J. Beynon and J. A. Wilson, J. Phys.: Condens. Matter **5**, 1983 (1993)
[6] A. Seidel and P. A. Lee (private communication).
[7] J. W. Bray, L. V. Iterrante, I. S. Jacobs, and J. C. Bonner, in *Extended Linear Chain Compounds*, edited by J. S. Miller (Plenum, NewYork, 1983), Chap. 7, pp. 353–415.
[8] G. Khaliullin and S. Maekawa, Phys. Rev. Lett. **85**, 3950 (2000).
[9] J. v. d. Brink, G. Khaliullin, and D. Khomskii, *Colossal Magnetoresistive Manganites*, edited by T. Chatterji (Kluwer Academic, Dordrecht, 2000).
[10] S. K. Pati, R. R. P. Singh, and D. I. Khomskii, Phys. Rev. Lett. **81**, 5406 (1998).
[11] Y. Yamashita, N. Shibata, and K. Ueda, J. Phys. Soc. Jpn. **69**, 242 (2000).
[12] A. K. Koleshuk, H.-J. Mikeska, and U. Schollwöck, Phys. Rev. B **63**, 064418 (2001).
[13] T. Imai and F. Chou, cond-mat/0301425.
[14] T. Saha-Dasgupta, R. Valentí, H. Rosner, and C. Gros, Europhys. Lett. **67**, 63 (2004).
[15] Y. S. Lee, E. Abel, and F. C. Chou (private communication).
[16] G. Caimi, L. Degiorgi, N. N. Kovaleva, P. Lemmens, and F. C. Chou, Phys. Rev. B **69**, 125108 (2004).
[17] P. Lemmens, G. Güntherodt, and C. Gros, Phys. Rep. **375**, 1

(2003).
[18] A. Damascelli, D. van der Marel, M. Grüninger, C. Presura, T. T. M. Palstra, J. Jegoudez, and A. Revcolevschi, Phys. Rev. Lett. **81**, 918 (1998).
[19] V. Kataev, J. Baier, A. Möller, L. Jongen, G. Meyer, and A. Freimuth, Phys. Rev. B **68**, 140405 (2003).
[20] P. Lemmens, K.-Y. Choi, E. E. Kaul, C. Geibel, K. Becker, W. Brenig, R. Valentí, C. Gros, M. Johnsson, P. Millet, and F. Mila, Phys. Rev. Lett. **87**, 227201 (2001).
[21] W. Brenig and K. W. Becker, Phys. Rev. B **64**, 214413 (2001).
[22] See, e.g., G. Blumberg, M. V. Klein, and S.-W. Cheong, Phys. Rev. Lett. **80**, 564 (1998); K. Yamamoto, T. Katsufuji, T. Tanaba, and Y. Tokura, *ibid.* **80**, 1493 (1998).
[23] K. P. Schmidt, C. Knetter, M. Grüninger, and G. S. Uhrig, Phys. Rev. Lett. **90**, 167201 (2003).
[24] A. Lanzara, P. V. Bogdanov, X. J. Zhou, S. A. Kellar, D. L. Feng, E. D. Lu, T. Yoshida, H. Eisaki, A. Fujimori, K. Kishio, J.-I. Shimoyama, T. Noda, S. Uchida, Z. Hussain, and Z.-X. Shen, Nature (London) **412**, 510 (2003).